Title

Zinc(II)-Tetradentate-Coordinated Probe with Aggregation-Induced Emission Characteristics for Selective Imaging and Photoinactivation of Bacteria

Journal

ACS Omega, 2(2)

ISSN

2470-1343

Authors

Feng, Guangxue
Zhang, Chong-Jing
Lu, Xianmao
et al.

Publication Date

2017-02-28

DOI

10.1021/acsomega.6b00564

Peer reviewed

ACS OMEGA

Article

http://pubs.acs.org/journal/acsodf

Zinc(II)-Tetradentate-Coordinated Probe with Aggregation-Induced Emission Characteristics for Selective Imaging and Photoinactivation of Bacteria

Guangxue Feng,[†,§] Chong-Jing Zhang,[†,§] Xianmao Lu,[†] and Bin Liu*[,†,‡]

[†]Department of Chemical and Biomolecular Engineering, National University of Singapore, 4 Engineering Drive 4, Singapore 117585

[‡]Institute of Materials Research and Engineering, Agency for Science, Technology and Research (A*STAR), 2 Fusionopolis Way, Singapore 138634

Supporting Information

ABSTRACT: The emergence of drug-resistant bacterial pathogens highlights an urgent need for new therapeutic options. Photodynamic therapy (PDT) has emerged as a potential alternative to antibiotics to kill bacteria, which has been used in clinical settings. PDT employs photosensitizers (PSs), light, and oxygen to kill bacteria by generating highly reactive oxygen species (ROS). PDT can target both external and internal structures of bacteria, which does not really require the PSs to enter bacteria. Therefore, bacteria can hardly develop resistance to PDT. However, most of the PSs reported so far are hydrophobic and tend to form aggregates when they interact with bacteria. The aggregation could cause fluorescence quenching and reduce ROS generation, which generally compromises the effects of both imaging and therapy. In this contribution, we report on a Zn(II)-tetradentate-coordinated red-emissive probe with aggregation-induced emission characterization. The probe could selectively image bacteria over mammalian cells. Moreover, the probe shows potent phototoxicity to both Gram-negative bacteria (*Escherichia coli*) and Gram-positive bacteria (*Bacillus subtilis*).

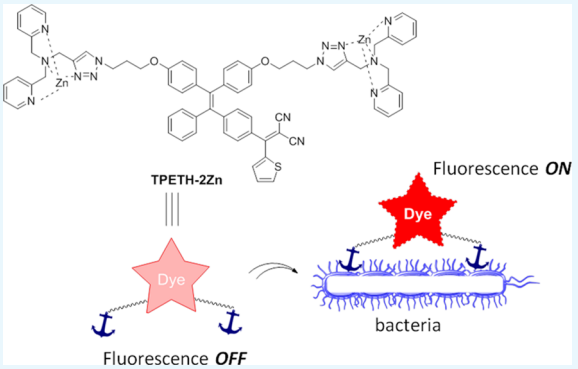

INTRODUCTION

The emergence of drug-resistant bacterial pathogens highlights an urgent need for new therapeutic options.[1] The dominant resistance mechanisms include alteration of antibiotic targets, active efflux of antibiotics from the cell, and antibiotic modification catalyzed by enzymes.[2] Many pathogens simultaneously harbor several mechanisms to achieve antibiotic resistance. One comprehensive approach to overcome resistance is to develop antibiotic adjuvants that contain both antibiotics and other bioactive molecules.[3] These adjuvants change the physiology of antibiotic-insensitive cells, incur a synergetic effect, and finally improve the treatment efficiency and inhibit resistance. The alternative choice is through photodynamic therapy (PDT). PDT has emerged as a good and potential alternative to antibiotics to kill bacteria that has been used in clinical settings.[4] PDT employs photosensitizers (PSs), light, and oxygen to kill bacteria by generating highly reactive oxygen species (ROS).[5] PDT can target both external and internal structures of bacteria, which does not really require the PSs to enter bacteria.[6] Therefore, bacteria can hardly develop resistance to PDT.[5a,7] In addition, many PSs could aid in image-guided antibacterial studies, as they also have intrinsic fluorescence. However, most of the PSs reported so far are hydrophobic and tend to form aggregates when they interact with bacteria. The aggregation could cause fluorescence quenching and reduce ROS generation,[8] which generally compromises the effects of both imaging and therapy.

Fluorogens with aggregation-induced emission (AIE) characteristics have recently attracted great attention in biological sensing, imaging, and therapeutic applications.[9] AIE fluorogens (AIEgens) generally show very weak fluorescence as free molecules but can become highly emissive in the aggregated state.[10] Moreover, strong ROS generation has been observed for some AIEgens, which are effective for cancer-cell ablation under light irradiation.[11] So far, several positively charged AIEgens have been reported to image and kill bacteria on the basis of electrostatic interactions.[12] To endow the probes with a positive charge, ammonium salts[13a] and the zinc(II)-dipicolylamine (ZnDPA) coordination complex[13b,c] are often employed, among which ZnDPA is the most popular as it has a stronger binding affinity with bacteria due to its higher positive charge.[13b,c] In our previous work, we developed a zinc(II)-coordinated PS (AIE-ZnDPA) with AIE and excited-state intramolecular proton transfer characteristics to selectively image and kill bacteria over mammalian cells.[14] Although successful, the probe has several limitations. First, the used

Received: December 29, 2016
Accepted: January 30, 2017
Published: February 14, 2017

DOI: 10.1021/acsomega.6b00564
ACS Omega 2017, 2, 546−553

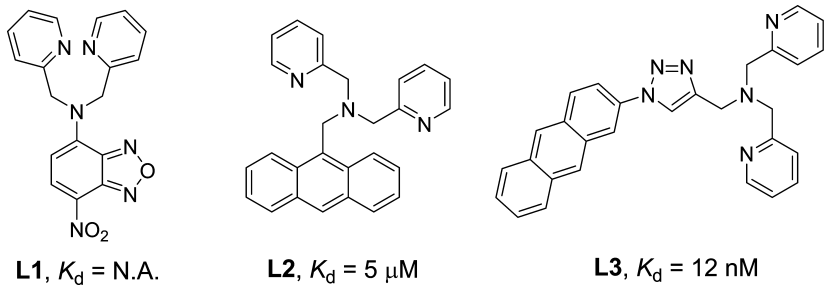

Figure 1. Selected zinc(II)-binding ligands and their apparent dissociation constants.

Scheme 1. Synthetic Route to the Probes

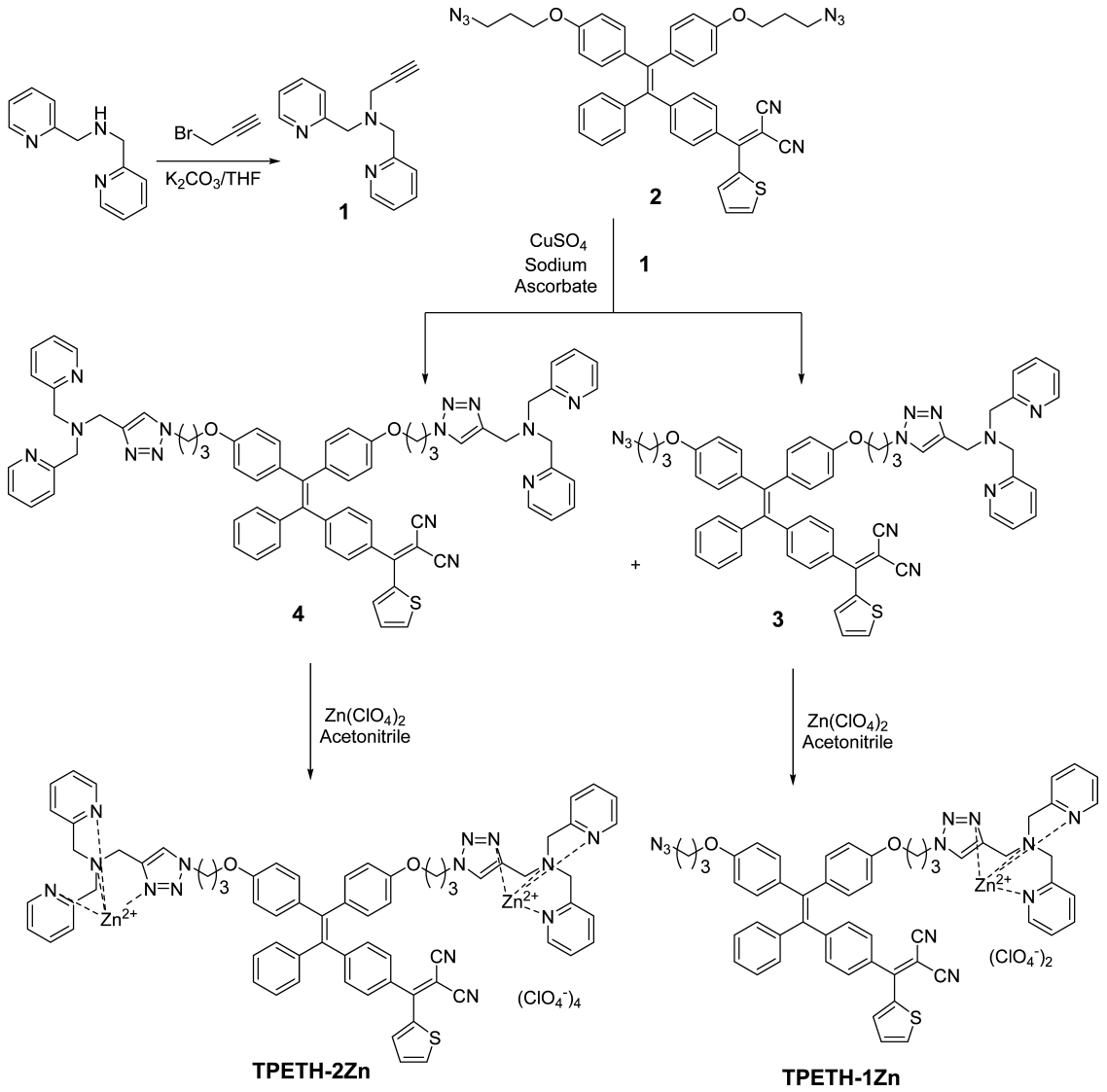

AIEgen absorbs mainly in the UV region, which makes it difficult for the probe to produce ROS when white light is used as the light source. Moreover, fluorogens with short-wavelength absorption and emission possess severe interference from sample autofluorescence.[15] Second, AIE-ZnDPA used DPA to coordinate zinc(II), which served as an anchor to the negatively charged bacterial membrane. However, the binding between DPA and zinc(II) is weak, with a K_d of around 5 μM (Figure 1).[16] As K_d is the ratio between ([free ligand] × [ion]) and [the ligand−ion binding complex], a higher K_d indicates that more free ligands exist in solution (eq 1 in Supporting Information). As the ligand−ion complex is the recognition element in the probe, a larger amount of probes are needed to bind with bacteria. This can also lead to a higher background signal, as more unbound free probes exist in the detection system. To design a better zinc(II)-binding ligand, we reviewed the literature and found that (1) electron-withdrawing groups can decrease the electron density on the ligand, which significantly reduces its binding affinity (L1 vs L2; Figure 1)[17] and that (2) additional binding positions could significantly increase the

DOI: 10.1021/acsomega.6b00564
ACS Omega 2017, 2, 546−553

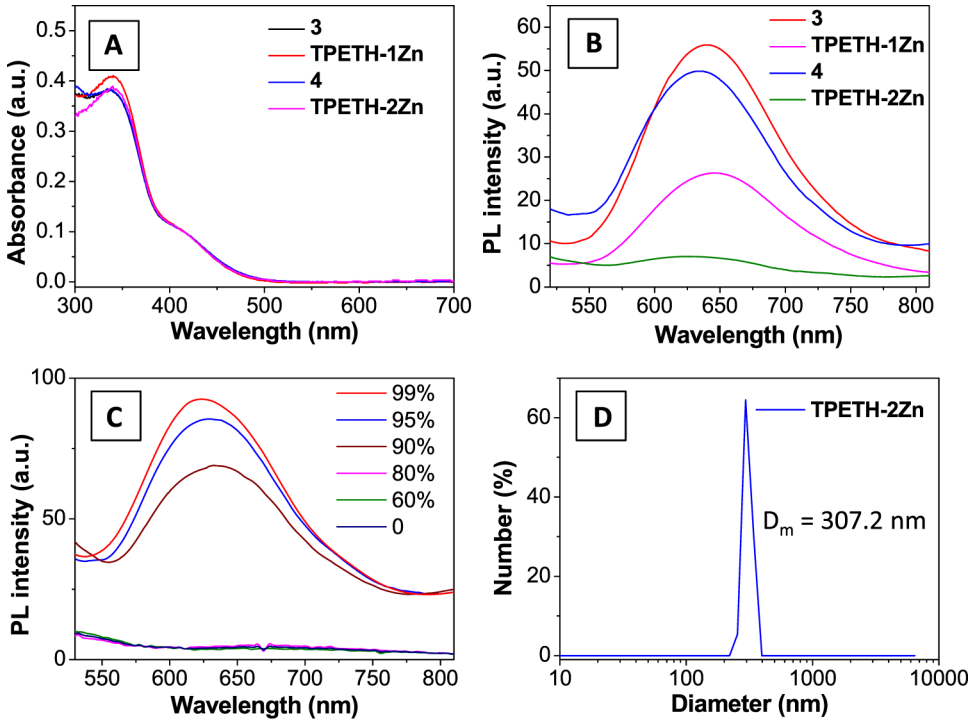

Figure 2. (A) Ultraviolet−visible (UV−vis) absorption spectra of **3**, **TPETH-1Zn**, **4**, and **TPETH-2Zn** in DMSO. (B) Photoluminescence (PL) spectra of **3**, **TPETH-1Zn**, **4**, and **TPETH-2Zn** in DMSO/water (v/v = 1/100). (C) PL spectra of **TPETH-2Zn** in a mixture of acetonitrile and ethyl ether, with various percentages of ethyl ether. (D) Hydrodynamic diameter measured with laser light scattering for **TPETH-2Zn** (10 μM) in a mixture of acetonitrile/ether (v/v = 1/100).

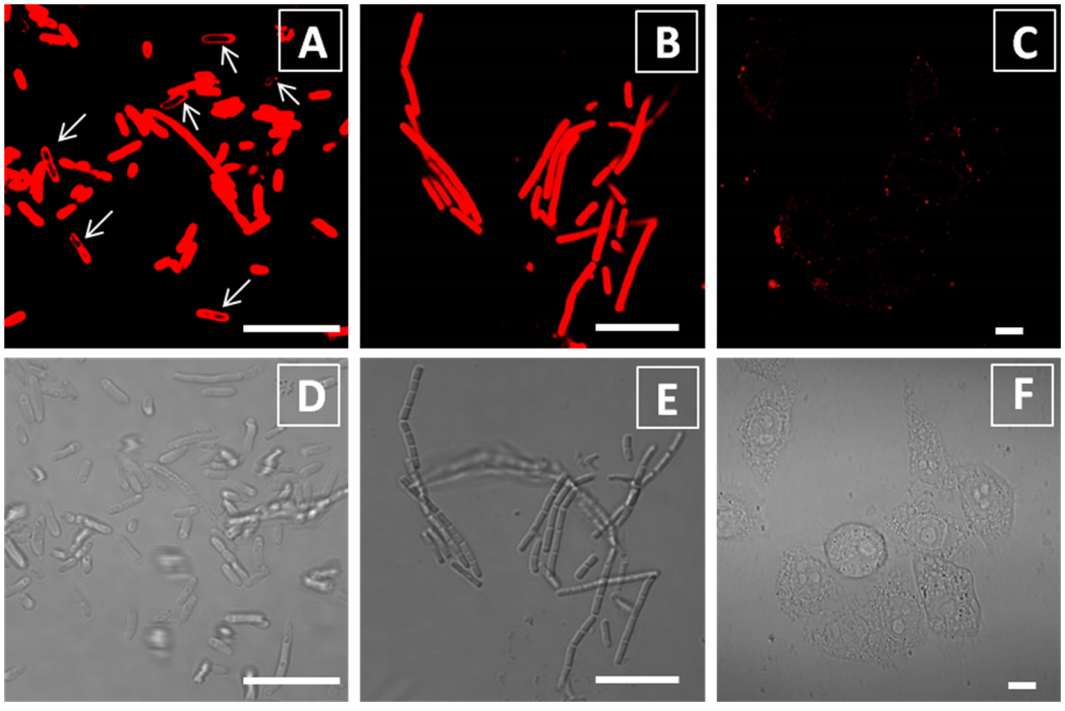

Figure 3. Confocal (A−C) and bright-field (D−F) images of *E. coli* (A, D) *B. subtilis* (B, E), and HeLa cells (C, F) after incubation with the **TPEPH-2Zn** probe (20 μM) for 30 min without any washing steps. The red signal is collected above 590 nm upon excitation at 458 nm. All images share the same scale bar of 10 μm.

binding affinity (L2 vs L3; Figure 1).[18] We are specifically interested in L3 because it could be readily synthesized by Cu(I)-catalyzed azide−alkyne cycloaddition (CuAAC) and shows a very low K_d value, in the nanomolar range.[18a] Taking all of the above considerations into account, in this work, we employ CuAAC to decorate a red-emissive AIE PS (TPETH) to develop a new probe for bacterial detection and killing. The probe is almost nonemissive in aqueous solution, but it becomes highly emissive after binding to the membrane of

DOI: 10.1021/acsomega.6b00564
ACS Omega 2017, 2, 546−553

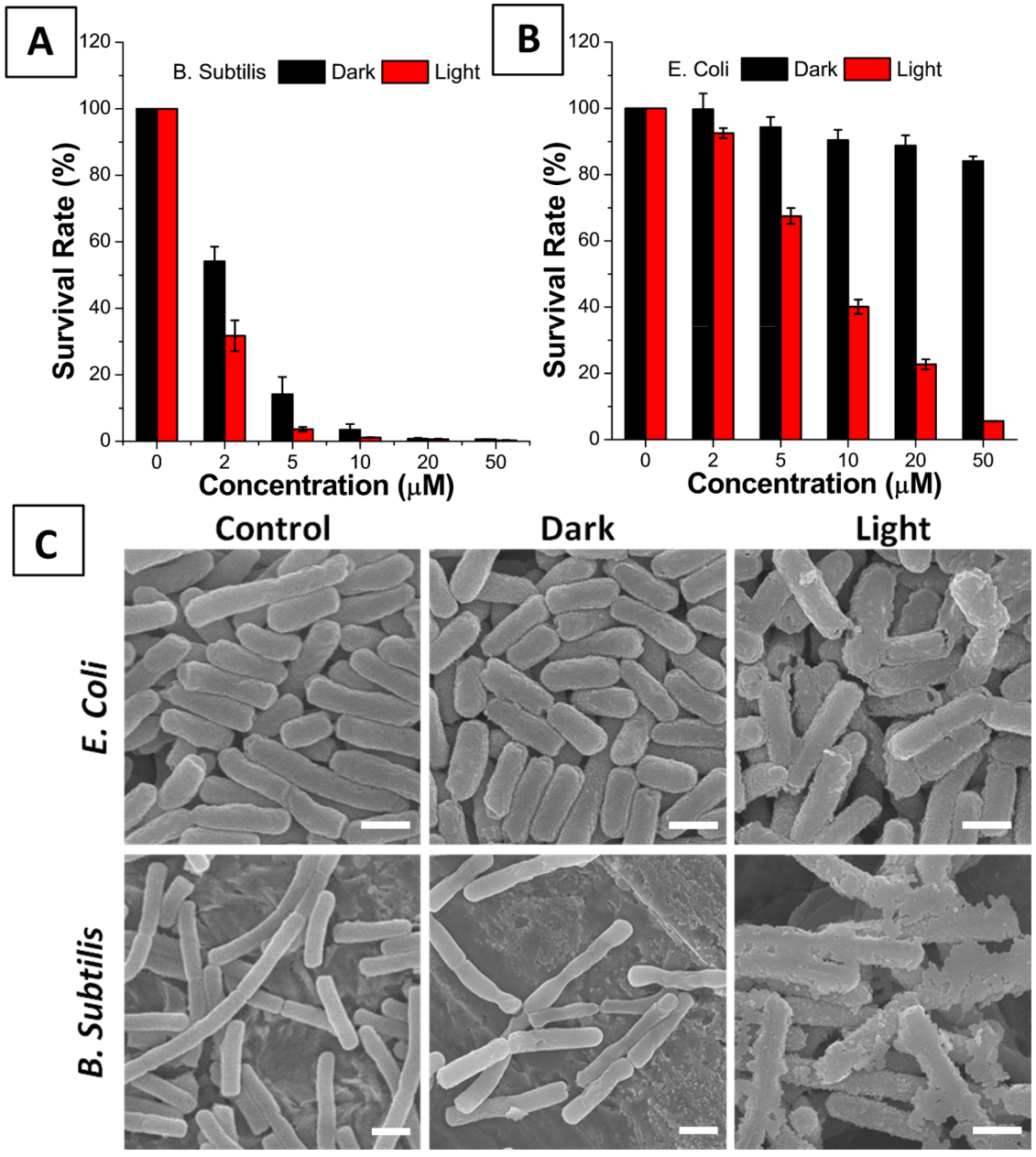

Figure 4. Survival rates of (A) *B. subtilis* and (B) *E. coli* treated with **TPEPH-2Zn** at different concentrations, with or without light irradiation. (C) SEM images of *E. coli* and *B. subtilis* treated with **TPEPH-2Zn**, with or without light irradiation. All images share the same scale bar of 1 μm.

bacteria. In addition, the probe can efficiently generate ROS to kill bacteria.

RESULTS AND DISCUSSION

The synthetic route to the probes is shown in Scheme 1. Briefly, alkylation of bis-2-picolylamine with propargyl bromide generated **1**. A CuAAC-mediated click reaction between **1** and **2** yielded intermediates **3**, with one binding motif, and **4**, with two binding motifs. Intermediates **3** and **4** were treated with zinc perchlorate to yield the probes **TPETH-1Zn** and **TPETH-2Zn**. All compounds were characterized by NMR and high-resolution mass spectrometry (HRMS) to confirm their high purities and right structures (Figures S1−S15).

With the probes and their intermediates at hand, we first measured their photophysical properties. Compounds **3**, **4**, **TPETH-1Zn**, and **TPETH-2Zn** have similar absorption spectra in dimethyl sulfoxide (DMSO) (Figure 2A). However, their fluorescent properties are very different. As shown in Figure 2B, **3** and **4** are highly emissive in the mixture of water and DMSO (v/v = 100/1), whereas **TPETH-1Zn** has moderate emission and **TPETH-2Zn** is only weakly emissive under the same conditions. This indicates that the binding between **3** or **4** and zinc(II) increases the probe solubility in aqueous media, leading to decreased background signals. The increased aqueous solubility after zinc(II) binding was further confirmed by dynamic light scattering experiments. Both **3** and **4** have a mean hydrodynamic diameter of around 300 nm, whereas **TPETH-1Zn** exhibits a mean size of around 30 nm after zinc(II) binding, but no hydrodynamic size can be detected for **TPETH-2Zn** (Figure S16), clearly indicating that zinc(II) binding could largely improve the aqueous solubility of the probe. Following this fluorescence change after binding

DOI: 10.1021/acsomega.6b00564
ACS Omega 2017, 2, 546−553

with zinc(II), we measured the dissociation constant (K_d) of **TPETH-1Zn** by fitting the fluorescence titration data with a 1:1 association equation (Figure S17A). The K_d is calculated to be 16.7 nM for **TPETH-1Zn** (Figure S17B), which indicates that the ligands in **TPETH-2Zn** can bind to Zn(II) tightly.

Although **TPETH-2Zn** is almost nonemissive in aqueous media, its fluorescence is intensified in the mixture of acetonitrile and ethyl ether when the ratio of ether increases (Figure 2C). When the ether-to-acetonitrile ratio is above 90%, **TPETH-2Zn** becomes insoluble and emits bright red fluorescence and forms aggregates with an average diameter of 307 nm (Figure 2D). These results indicate that **TPETH-2Zn** is an AIEgen, which could turn on its fluorescence upon aggregate formation, such as upon binding to a bacterial surface.

After confirming that **TPETH-2Zn** was not emissive in aqueous medium but was able to fluoresce upon aggregate formation, we evaluated its performance in real-time imaging of bacteria. Without any washing steps, the probe emits strong red emission upon interaction with bacteria (*Escherichia coli* and *Bacillus subtilis*), which is significantly brighter than that in PBS only (Figure S18). The fluorescence increase is dependent on the probe concentration. The confocal image (Figure 3) indicates that both *E. coli* and *B. subtilis* are stained by **TPETH-2Zn** after 30 min of incubation. It is noted that no washing is required for image acquisition. For *B. subtilis*, the probe lights up the whole bacterial cell, including the membrane and inner parts. For *E. coli*, although the probe stains the whole bacterial cell in the majority of *E. coli*, it stains only the membrane in some *E. coli* (arrow in Figure 3A). This small difference indicates that it is easier for the probe to penetrate into *B. subtilis* than into *E. coli*, as the latter contains an extra outer membrane.[19] On the other hand, **TPETH-2Zn** only slightly stains HeLa cells under the same conditions (Figures 3C and S19), indicating that the probe prefers bacteria to mammalian cells. Together, these data demonstrate that *E. coli* and *B. subtilis*, with negatively charged membranes, could anchor, uptake, and aggregate the positively charged probe, which restricts the intramolecular motion, leading to fluorescence.

As reported, TPETH also has good efficiency to generate singlet oxygen species ($^1O_2$) under light irradiation.[20] Next, we tested whether **TPETH-2Zn** has a similar ability to generate singlet oxygen. 9,10-Anthracenediylbis(methylene)dimalonic acid (ABDA), which quickly decomposes upon reaction with $^1O_2$, was used as an indicator of $^1O_2$ generation. White light irradiation of the mixture of **TPETH-2Zn** and ABDA in water greatly diminishes the absorbance of ABDA. After light irradiation for 2 min, around 90% of ABDA was consumed (Figure S20). The singlet oxygen quantum yield for **TPETH-2Zn** is 77.6%, measured using Rose Bengal as the reference.[21] It should be noted that **TPETH-2Zn** exhibited a similar singlet oxygen generation ability even after binding to bacteria (Figure S21), indicating that the design of AIE PS could offer an effective singlet oxygen generation ability in the aggregated state.

Finally, we applied **TPETH-2Zn** to photoablate bacteria. In the dark, the probe shows little toxicity toward *E. coli* but high toxicity toward *B. subtilis*, as 20 μM **TPETH-2Zn** could kill nearly all of the *B. subtilis* but only less than 10% of the *E. coli* (Figure 4A,B). The same trend was also observed in our previous report, mainly because *E. coli* contains an extra outer protective membrane as an effective barrier to PSs.[14,19] Under irradiation with white light (100 mW cm^{-2}), 10 μM **TPETH-2Zn** could photoinactivate all of the *B. subtilis* and 60% of the *E. coli* (Figures 4A,B, S22, and S23). Scanning electron microscopy (SEM) results indicate that the membranes of bacteria are damaged after probe treatment and light irradiation (Figure 4C). It should be noted that under the same experimental conditions the previous probe (AIE-ZnDPA, 10 μM) could only photoinactivate about 80% of the *B. subtilis* and 10% of the *E. coli*, which is around fivefold less toxicity than that of **TPETH-2Zn**. This toxicity difference could partially be ascribed to the lower K_d of **TPETH-2Zn** than that of AIE-ZnDPA, which favors bacterial binding in this case. It should be noted that **TPETH-2Zn** could not cause any dark or light toxicity toward HeLa cells (Figure S24), indicating that the AIE probe could selectively kill bacteria over mammalian cells due to the different binding affinities.

CONCLUSIONS

In conclusion, we used click chemistry (CuAAC) to readily synthesize a light-up AIE probe (**TPETH-2Zn**) that tightly binds zinc(II), selectively images bacteria over mammalian cells, and potently exerts phototoxicity to bacteria. The AIE probe, **TPETH-2Zn**, is not emissive in aqueous solution but is able to turn on its emission upon aggregate formation. As most bacteria contain significant amounts of anionic phospholipids, which make their membrane negatively charged,[22] **TPETH-2Zn** could tightly bind to the bacterial surface, but not mammalian cell membranes, and fluoresce. Benefiting from its low background signal, **TPETH-2Zn** does not require additional washing steps, which largely simplifies the imaging procedure and detection sensitivity. Possessing excellent singlet oxygen generation ability even after binding to bacteria, **TPETH-2Zn** potentially serves as an effective theranostic probe for killing bacteria, which shall open new opportunities for the treatment of bacterial infections.

METHODS

Materials and Instruments. All the chemicals were purchased from a commercial vendor and used directly without further purification. Dry dichloromethane was distilled over CaH_2. All ^{1}H NMR and ^{13}C NMR spectra were recorded on a Bruker ACF-400 MHz NMR spectrometer with $CDCl_3$ or $(CD_3)_2SO$ (DMSO-d_6) as the solvent. Chemical shifts are described in parts per million, which are referenced according to residual solvent for ^{1}H NMR (7.26 ppm for $CDCl_3$ and 2.50 ppm for DMSO-d_6) and ^{13}C NMR (77.0 ppm for $CDCl_3$ and 40.0 ppm for DMSO-d_6). HRMS (ESI) spectra were recorded by the AmaZon X LC-MS. UV−vis absorption spectra were recorded on a Shimadzu Model UV-1700 spectrometer. PL spectra were recorded on a Perkin-Elmer LS 55 spectrofluorometer.

Synthesis of 3 and 4. To the solution of **1** (60 mg, 0.087 mmol) and **2** (50 mg, 0.21 mmol) in DMSO (2.0 mL) were added copper sulfite (1.6 mg, 0.01 mmol) and sodium ascorbate (4.0 mg, 0.02 mmol) in water (0.1 mL). The mixture was stirred at room temperature for 24 h. Then, water (20 mL) was added to quench the reaction. The precipitated solid was purified by chromatography to give product **4** as a red oil (5.0 mg). ^{1}H NMR (400 MHz, $CDCl_3$) δ 8.59 (m, 4H), 7.82 (dd, J_1 = 1.2 Hz, J_2 = 4.8 Hz, 1H), 7.71−7.74 (m, 4H), 7.64−7.65 (m, 3H), 7.11−7.24 (m, 11 H), 7.03−7.06 (m, 2H), 6.87−6.94 (m, 4H), 6.60−6.64 (m, 4H), 4.56 (t, J = 6.8 Hz, 4H), 4.11−4.14 (m, 12H), 3.92 (m, 4H), 2.34−2.37 (m, 4H); HRMS (ESI) calcd for $[M + Na]^+$: 1185.4793, found: 1185.4795. Product **3**

DOI: 10.1021/acsomega.6b00564
ACS Omega 2017, 2, 546−553

is a red oil (20 mg). ^{1}H NMR (400 MHz, $CDCl_3$) δ 8.53 (m, 2H), 7.79−7.81 (m, 1H), 7.72 (m, 1H), 7.62−7.66 (m, 3H), 7.55−7.57 (m, 2H), 7.11−7.19 (m, 9H), 7.04−7.04 (m, 2H), 6.88−6.95 (m, 4H), 6.61−6.65 (m, 4H), 4.53 (t, J = 6.8 Hz, 2H), 3.97 (t, J = 5.6 Hz, 2H), 3.87−3.93 (m, 8H), 3.48 (t, J = 6.8 Hz, 2H), 2.33−2.36 (m, 2H), 1.99−2.02 (m, 2H); HRMS (ESI) calcd for $[M + H]^+$: 926.3708, found: 926.3704.

Synthesis of TPETH-1Zn. To the solution of **3** (1.9 mg) in acetonitrile (2.0 mL) was added zinc perchlorate hexahydrate (0.82 mg). The mixture was stirred at room temperature for 30 min. Then, all of the solvent was removed under reduced pressure to give the product without further purification. ^{1}H NMR (400 MHz, CD_3CN) δ 8.72 (m, 2H), 8.10−8.15 (tt, J_1 = 1.2 Hz, J_2 = 7.6 Hz, 2H), 7.97−8.00 (m, 1H), 7.94 (m, 1H), 7.65−7.68 (m, 3H), 7.58−7.60 (m, 2H), 7.21−7.29 (m, 3H), 7.13−7.1 (m, 5H), 7.05−7.08 (m, 2H), 6.93−6.95 (m, 1H), 6.87−6.90 (m, 2H), 6.80−6.82 (m, 1H), 6.69−6.71 (m, 2H), 6.53−6.55 (m, 2H), 4.58−4.62 (m, 2H), 4.23 (s, 4H), 3.95−3.99 (dt, J_1 = 1.2 Hz, J_2 = 6.0 Hz, 2H), 3.95 (t, J = 6.0 Hz, 2H), 3.41−3.48 (m, 2H), 2.30 (m, 2H); HRMS (ESI) calcd for $[M - ClO_4]^+$: 1088.2406, found: 1088.2401.

Synthesis of TPETH-2Zn. To the solution of **4** (5.0 mg) in acetonitrile (2.0 mL) was added zinc perchlorate hexahydrate (2.3 mg). The mixture was stirred at room temperature for 30 min. Then, all of the solvent was removed under reduced pressure to give the product without further purification. ^{1}H NMR (400 MHz, CD_3CN) δ 9.02 (brs, 4H), 8.06 (m, 4H), 7.98 (dd, J_1 = 1.2 Hz, J_2 = 5.2 Hz, 2H), 7.92 (m, 2H), 7.62−7.66 (m, 5H), 7.53 (d, J = 7.6 Hz, 3H), 7.22−7.26 (m, 3H), 7.10−7.18 (m, 6H), 7.03−7.06 (m, 2H), 6.76−6.85 (m, 4H), 6.54−6.56 (m, 4H), 4.62 (m, 4H), 4.16 (brs, 8H), 4.02 (brs, 4H), 3.95 (m, 4H); HRMS (ESI) calcd for $[M - 2ClO_4]^{2+}$: 744.1222, found: 744.1221.

Bacterial Labeling. The bacterial suspensions (*E. coli* or *B. subtilis*) at an OD600 of 0.2 in 1× phosphate buffered saline (PBS) buffer were incubated with **TPETH-2Zn** (20 μM) for 30 min at room temperature. After incubation, the bacteria were harvested by centrifugation at 5000 rpm for 5 min, the unbound **TPETH-2Zn** in the supernatant was discarded, and the bacteria were re-suspended in PBS buffer for absorbance measurements. To study the fluorescence of **TPETH-2Zn** upon binding to bacteria, these bacteria were transferred to a 96-well plate in a volume of 100 μL/well, with an OD600 of 0.1. Designated concentrations of **TPETH-2Zn** were then added into each well. After 30 min of incubation, the fluorescence intensity at 650 nm upon excitation at 458 nm was recorded. PBS was used as a negative control.

Confocal Imaging Experiments. The prepared bacterial (*B. subtilis* and *E. coli*) solutions were incubated with 20 μM **TPETH-2Zn** in the dark for 30 min at 37 °C. Individual aliquots of 10 μL of the prepared suspension were spotted on polylysine-pretreated glass slides and immobilized with coverslips. The specimens were imaged immediately under a confocal laser scanning microscope (CLSM; Zeiss). Excitation wavelength: 458 nm (1% laser power); emission filter: LP590 nm. For confocal images of HeLa cells, the HeLa cells were seeded in an eight-well chamber at 4 × 10^4 cells/mL. After overnight culturing, the HeLa cells were incubated with **TPETH-2Zn** at a concentration of 20 μM for 30 min. The cells were immediately imaged under a CLSM without washing, using the same setup for bacterial imaging.

Antimicrobial Assay. The antibacterial activity of **TPETH-2Zn** was studied by plating the diluted bacterial suspensions on a solid Luria−Bertani (LB) agar plate. The bacteria were harvested and re-suspended in 1× PBS with an OD600 of 0.5. Then, 90 μL of the bacterial suspension was added to a 96-well plate and **TPETH-2Zn** was added to each well to achieve final concentrations of 0, 2, 5, 10, 20, and 50 μM. The total volume was kept at 100 μL, and the plate was incubated in the dark at 37 °C for 30 min. For the photodynamic antibacterial assay, the samples in the 96-plate were illuminated with white light for 5 min at 100 mW cm^{-2}. After irradiation, the bacterial suspensions were serially diluted 0.5−1 × 10^5-fold with 1× PBS. A portion (100 μL) of the diluted bacterial cells was spread on the solid LB agar plate and incubated at 37 °C for 16 h. The colonies formed were counted, and the survival rates of the bacteria were determined from colony-forming unit counting on the solid LB agar plate with the control in the dark without **TPETH-2Zn** treatment. For the control in the dark, the irradiation step was replaced by incubation in the dark for 6 min.

SEM Measurements. On the basis of the antimicrobial experiments, the concentration of **TPETH-2Zn** was determined to be 20 μM for SEM measurements. The bacteria were centrifuged at 5000 rpm for 5 min to remove the 1× PBS, followed by irradiation. They were then suspended in and fixed with 2.5% glutaraldehyde for 2−3 h at room temperature. The glutaraldehyde was removed by centrifugation, and the bacterial pellets were re-suspended in sterile water; then, 10 μL of the bacterial suspension was spotted onto the SEM conducting paste. After natural drying in air, the bacteria were dehydrated with a series of graded ethanol solutions (30, 50, 70, 80, 90, and 100% for 6 min). After drying overnight, the specimens were coated with platinum before SEM measurements.

■ ASSOCIATED CONTENT

Supporting Information

The Supporting Information is available free of charge on the ACS Publications website at DOI: 10.1021/acsomega.6b00564.

Synthesis of compounds **1** and **2**; preparation of the bacterial solution and cell culture; binding constant determination; ^{1}H NMR, ^{13}C NMR, and HRMS spectra; fluorometric titration of **3** with $ZnSO_4$; hydrodynamic diameters of **3**, **4**, and **TPETH-1Zn** in aqueous media; time-dependent bleaching of ADPA caused by **TPETH-2Zn** with white light irradiation, with or without the presence of bacteria; plate photographs of *E. coli* and *B. subtilis* on LB agar plates supplemented with **TPETH-2Zn**, with or without white light irradiation; cell viability of **TPETH-2Zn**-treated HeLa cells, with or without white light irradiation (PDF)

■ AUTHOR INFORMATION

Corresponding Author

*E-mail: cheliub@nus.edu.sg.

ORCID

Xianmao Lu: 0000-0002-7422-2867

Bin Liu: 0000-0002-0956-2777

Author Contributions

§G.F. and C.-J.Z. contributed equally to this work.

Author Contributions

The manuscript was written through contributions of all authors. All authors have given approval to the final version of the manuscript.

DOI: 10.1021/acsomega.6b00564
ACS Omega 2017, 2, 546−553

Notes

The authors declare no competing financial interest.

■ ACKNOWLEDGMENTS

The authors thank SMART (R279-000-378-592), the Ministry of Education (R279-000-391-112), Singapore NRF Investigatorship (R279-000-444-281), and the Institute of Materials Research and Engineering of Singapore (IMRE/14-8P1110) for financial support.

■ REFERENCES

(1) (a) Arias, C. A.; Murray, B. E. Antibiotic-Resistant Bugs in the 21st Century — A Clinical Super-Challenge. *N. Engl. J. Med.* **2009**, 439−443. (b) Livermore, D. M. Has the era of untreatable infections arrived? *J. Antimicrob. Chemother.* **2009**, *64*, i29−i36.

(2) Blair, J. M. A.; Webber, M. A.; Baylay, A. J.; Ogbolu, D. O.; Piddock, L. J. V. Molecular mechanisms of antibiotic resistance. *Nat. Rev. Microbiol.* **2015**, *13*, 42−51.

(3) (a) Kalan, L.; Wright, G. D. Antibiotic adjuvants: multicomponent anti-infective strategies. *Expert Rev. Mol. Med.* **2011**, *13*, No. e5. (b) Gonzales, P. R.; Pesesky, M. W.; Bouley, R.; Ballard, A.; Biddy, B. A.; Suckow, M. A.; Wolter, W. R.; Schroeder, V. A.; Burnham, C. D.; Mobashery, S.; Chang, M.; Dantas, G. Synergistic, collaterally sensitive β-lactam combinations suppress resistance in MRSA. *Nat. Chem. Biol.* **2015**, *11*, 855.

(4) Taylor, P. W.; Stapleton, P. D.; Luzio, J. P. New ways to treat bacterial infections. *Drug Discovery Today* **2002**, *7*, 1086−1091.

(5) (a) Tavares, A.; Carvalho, C. M. B.; Faustino, M. A.; Neves, M. G. P. M. S.; Tomé, J. P. C.; Tomé, A. C.; Cavaleiro, J. A. S.; Cunha, Â.; Gomes, N. C. M.; Alves, E.; Almeida, A. Antimicrobial Photodynamic Therapy: Study of Bacterial Recovery Viability and Potential Development of Resistance after Treatment. *Mar. Drugs* **2010**, *8*, 91−105. (b) Shao, Q.; Xing, B. Enzyme responsive luminescent ruthenium(II) cephalosporin probe for intracellular imaging and photoinactivation of antibiotics resistant bacteria. *Chem. Commun.* **2012**, *48*, 1739−1741.

(6) Almeida, A.; Faustino, M. A. F.; Tomé, J. P. C. Photodynamic inactivation of bacteria: finding the effective targets. *Future Med. Chem.* **2015**, *7*, 1221−1224.

(7) (a) Maisch, T. Revitalized Strategies Against Multi-Resistant Bacteria: Antimicrobial Photodynamic Therapy and Bacteriophage Therapy. *Anti-Infect. Agents Med. Chem.* **2007**, *6*, 145−150. (b) Maisch, T. A New Strategy to Destroy Antibiotic Resistant Microorganisms: Antimicrobial Photodynamic Treatment. *Mini-Rev. Med. Chem.* **2009**, *9*, 974−983.

(8) (a) Bennett, L. E.; Ghiggino, K. P.; Henderson, R. W. Singlet oxygen formation in monomeric and aggregated porphyrin *c*. *J. Photochem. Photobiol., B* **1989**, *3*, 81−89. (b) Park, S. Y.; Baik, H. J.; Oh, Y. T.; Oh, K. T.; Youn, Y. S.; Lee, E. S. A Smart Polysaccharide/Drug Conjugate for Photodynamic Therapy. *Angew. Chem., Int. Ed.* **2011**, *50*, 1644−1647.

(9) (a) Shi, H.; Kwok, R. T. K.; Liu, J.; Xing, B.; Tang, B. Z.; Liu, B. Real-Time Monitoring of Cell Apoptosis and Drug Screening Using Fluorescent Light-Up Probe with Aggregation-Induced Emission Characteristics. *J. Am. Chem. Soc.* **2012**, *134*, 17972−17981. (b) Chen, S.; Hong, Y.; Liu, Y.; Liu, J.; Leung, C. W. T.; Li, M.; Kwok, R. T. K.; Zhao, E.; Lam, J. W. Y.; Yu, Y.; Tang, B. Z. Full-Range Intracellular pH Sensing by an Aggregation-Induced Emission-Active Two-Channel Ratiometric Fluorogen. *J. Am. Chem. Soc.* **2013**, *135*, 4926−4929. (c) Li, Y.; Yu, H.; Qian, Y.; Hu, J.; Liu, S. Amphiphilic Star Copolymer-Based Bimodal Fluorogenic/Magnetic Resonance Probes for Concomitant Bacteria Detection and Inhibition. *Adv. Mater.* **2014**, *26*, 6734−6741. (d) Hu, F.; Huang, Y.; Zhang, G.; Zhao, R.; Yang, H.; Zhang, D. Targeted Bioimaging and Photodynamic Therapy of Cancer Cells with an Activatable Red Fluorescent Bioprobe. *Anal. Chem.* **2014**, *86*, 7987−7995.

(10) (a) Ding, D.; Li, K.; Liu, B.; Tang, B. Z. Bioprobes Based on AIE Fluorogens. *Acc. Chem. Res.* **2013**, *46*, 2441. (b) Liang, J.; Tang, B. Z.; Liu, B. Specific light-up bioprobes based on AIEgen conjugates. *Chem. Soc. Rev.* **2015**, *44*, 2798−2811.

(11) (a) Zhang, C.-J.; Hu, Q.; Feng, G.; Zhang, R.; Yuan, Y.; Lu, X.; Liu, B. Image-guided combination chemotherapy and photodynamic therapy using a mitochondria-targeted molecular probe with aggregation-induced emission characteristics. *Chem. Sci.* **2015**, *6*, 4580−4586. (b) Yuan, Y.; Zhang, C.-J.; Gao, M.; Zhang, R.; Tang, B. Z.; Liu, B. Specific Light-Up Bioprobe with Aggregation-Induced Emission and Activatable Photoactivity for the Targeted and Image-Guided Photodynamic Ablation of Cancer Cells. *Angew. Chem., Int. Ed.* **2015**, *54*, 1780−1786.

(12) (a) Zhao, E.; Chen, Y.; Wang, H.; Chen, S.; Lam, J. W. Y.; Leung, C. W. T.; Hong, Y.; Tang, B. Z. Light-Enhanced Bacterial Killing and Wash-Free Imaging Based on AIE Fluorogen. *ACS Appl. Mater. Interfaces* **2015**, *7*, 7180−7188. (b) Feng, G.; Yuan, Y.; Hu, F.; Zhang, R.; Xing, B.; Zhang, G.; Zhang, D.; Liu, B. A light-up probe with aggregation-induced emission characteristics (AIE) for selective imaging, naked-eye detection and photodynamic killing of Gram-positive bacteria. *Chem. Commun.* **2015**, *51*, 12490−12493.

(13) (a) Maisch, T.; Bosl, C.; Szeimies, R.-M.; Lehn, N.; Abels, C. Photodynamic Effects of Novel XF Porphyrin Derivatives on Prokaryotic and Eukaryotic Cells. *Antimicrob. Agents Chemother.* **2005**, *49*, 1542−1552. (b) Leevy, W. M.; Johnson, J. R.; Lakshmi, C.; Morris, J.; Marquez, M.; Smith, B. D. Selective recognition of bacterial membranes by zinc(II)-coordination complexes. *Chem. Commun.* **2006**, *42*, 1595−1597. (c) Leevy, W. M.; Gammon, S. T.; Jiang, H.; Johnson, J. R.; Maxwell, D. J.; Jackson, E. N.; Marquez, M.; Piwnica-Worms, D.; Smith, B. D. Optical Imaging of Bacterial Infection in Living Mice Using a Fluorescent Near-Infrared Molecular Probe. *J. Am. Chem. Soc.* **2006**, *128*, 16476−16477.

(14) Gao, M.; Hu, Q.; Feng, G.; Tomaczak, N.; Liu, R.; Xing, B.; Tang, B. Z.; Liu, B. A Multifunctional Probe with Aggregation-Induced Emission Characteristics for Selective Fluorescence Imaging and Photodynamic Killing of Bacteria Over Mammalian Cells. *Adv. Healthcare Mater.* **2015**, *4*, 659−663.

(15) (a) Guo, Z.; Zhu, W.; Tian, H. Dicyanomethylene-4H-pyran chromophores for OLED emitters, logic gates and optical chemosensors. *Chem. Commun.* **2012**, *48*, 6073−6084. (b) Wang, X.; Morales, A. R.; Urakami, T.; Zhang, L.; Bondar, M. V.; Komatsu, M.; Belfield, K. D. Folate Receptor-Targeted Aggregation-Enhanced Near-IR Emitting Silica Nanoprobe for One-Photon in Vivo and Two-Photon ex Vivo Fluorescence Bioimaging. *Bioconjugate Chem.* **2011**, *22*, 1438−1450.

(16) de Silva, S. A.; Zavaleta, A.; Baron, D. E.; Allam, O.; Isidor, E. V.; Kashimura, N.; Percarpio, J. M. A fluorescent photoinduced electron transfer sensor for cations with an off-on-off proton switch. *Tetrahedron Lett.* **1997**, *38*, 2237−2240.

(17) Atilgan, S.; Ozdemir, T.; Akkaya, E. U. A Sensitive and Selective Ratiometric Near IR Fluorescent Probe for Zinc Ions Based on the Distyryl−Bodipy Fluorophore. *Org. Lett.* **2008**, *10*, 4065−4067.

(18) (a) Huang, S.; Clark, R. J.; Zhu, L. Highly Sensitive Fluorescent Probes for Zinc Ion Based on Triazolyl-Containing Tetradentate Coordination Motifs. *Org. Lett.* **2007**, *9*, 4999−5002. (b) Walkup, G. K.; Burdette, S. C.; Lippard, S. J.; Tsien, R. Y. A New Cell-Permeable Fluorescent Probe for Zn^{2+}. *J. Am. Chem. Soc.* **2000**, *122*, 5644−5645.

(19) (a) Wu, T.; McCandlish, A. C.; Gronenberg, L. S.; Chng, S. S.; Silhavy, T. J.; Kahne, D. Identification of a protein complex that assembles lipopolysaccharide in the outer membrane of *Escherichia coli*. *Proc. Natl. Acad. Sci. U.S.A.* **2006**, *103*, 11754−11759. (b) Pereira, M. A.; Faustino, M. A. F.; Tomé, J. P. C.; Neves, M. G. P. M. S.; Tomé, A. C.; Cavaleiro, J. A. S.; Cunha, Â.; Almeida, A. Influence of external bacterial structures on the efficiency of photodynamic inactivation by a cationic porphyrin. *Photochem. Photobiol. Sci.* **2014**, *13*, 680−690.

(20) Yuan, Y.; Zhang, C.-J.; Kwok, R. T. K.; Xu, S.; Zhang, R.; Wu, J.; Tang, B. Z.; Liu, B. Light-Up Probe for Targeted and Activatable Photodynamic Therapy with Real-Time In Situ Reporting of Sensitizer Activation and Therapeutic Responses. *Adv. Funct. Mater.* **2015**, *25*, 6586−6595.

DOI: 10.1021/acsomega.6b00564
ACS Omega 2017, 2, 546−553

(21) Xu, S.; Yuan, Y.; Cai, X.; Zhang, C.-J.; Hu, F.; Liang, J.; Zhang, G.; Zhang, D.; Liu, B. Tuning the singlet-triplet energy gap: a unique approach to efficient photosensitizers with aggregation-induced emission (AIE) characteristics. *Chem. Sci.* **2015**, *6*, 5824−5830.
(22) Ratledge, C.; Wilkinson, S. G. *Microbial Lipids*; Academic Press: New York, 1988.

DOI: 10.1021/acsomega.6b00564
ACS Omega 2017, 2, 546−553